Semi-supervised Cloud Edge Collaborative Power Transmission Line Insulator Anomaly Detection Framework

Yanqing Yang[1], Jianxu Mao[1], Hui Zhang[1(✉)], Yurong Chen[1], Hang Zhong[1], Zhihong Huang[2], and Yaonan Wang[1]

[1] National Engineering Laboratory of Robot Visual Perception and Control Technology, Hunan University, Changsha, Hunan, China
[2] State Grid Hunan Electric Power Corporation Limited Research Institute, Changsha, Hunan, China

Abstract. The widely deployed power transmission line expedites developing the age of electricity. Thus, it is necessary to maintain a power system with a great quantity of manpower and material resources, especially for crucial equipment, such as insulator string. However, the current main inspection method relies on artificial with the problem of time-consuming and labor-intensive. There is a trend of utilizing deep learning techniques on unmanned aerial vehicles (UAVs) to accomplish the inspection task, but its development is restricted by the limitation of energy. In this paper, we propose a semi-supervised cloud edge collaborative insulator string anomaly detection framework. Specifically, an anchor-free object detector is deployed on the edge device for locating the insulator. On the cloud side, we propose a generative insulator defect detection model based on the autoencoder (AE) with a generator-discriminator pattern. Particularly, we introduce the variational memory encoder-decoder architecture to model defect-free insulator data distribution. Furthermore, the adversarial strategy is employed to regularize the generated data space with input data space. In the end, the anomaly can be detected if its data space is an outlier of training defect-free distribution. Comprehensive experiments demonstrate that our method can effectively reduce the computational load, meanwhile archiving superior performance, including accuracy (0.968) and recall (0.985), for defect recognition using a standard insulator data set.

Keywords: Insulator detection · Defect recognition · Autoencoder

1 Introduction

The transmission line connects power plants, substations, and users to form a transmission grid and a distribution network, and its status greatly influences the safety and reliable operation of the whole power system. Accordingly, the condition monitoring for transmission lines has always been the focus of attention,

Y. Peng et al. (Eds.): ICIG 2021, LNCS 12888, pp. 210–221, 2021.
https://doi.org/10.1007/978-3-030-87355-4_18

especially for the main component such as the insulator string. Insulator plays a conductor insulation and mechanical support function in the power transmission task, yet vulnerable due to the long-term exposure in the external environment. And a plenty of fact proof that insulator failure is the main reason causing the electrical accidents [1]. Moreover, it is challenging to screen the status of insulators, since deployed on high-voltage lines with strong currents. The traditional manual inspection method is cumbersome and inefficient, which need to blackout first, and then the staff members are supposed to climb to the position of insulator for checking its condition [1]. Thus, researchers and developers make a lot of effort on designing techniques of insulator string anomaly detection tasks.

Last few years, appreciating the maturity of Micro-Electro-Mechanical Systems (MEMS) techniques, people have witnessed unprecedented developments of the unmanned aerial vehicles (UAVs) field [2,3]. UAVs equipped with cameras can obtain a large amount of insulator image data, however, the lack of automatic status monitoring of insulator string methods brings a heavy burden workload of the developers. It is impractical to manually identifying defective insulators from such an enormous data source. In this case, a series of methods have been proposed for insulator detection and fault recognition, and they can be generally divided into two categories: (1) traditional image processing-based techniques [4,5]; (2) deep learning-based [6,7] algorithms. The former methods commonly make use of factors like color, shape, and texture features to analyze the insulator string, but limited by the sensitivity to the complex background and hard to get a trade-off between the detection speed and accuracy [1]. On the other hand, deep learning is an overwhelming technique on industrial of things [8,9]. There are many works that utilize deep convolutional neural networks (DCNNs) to inspect the equipment condition of the transmission line. Such as Zhao et al. [10] represent the insulator status by applying a multi-patch CNN feature extraction method, and [6] proposes a cascading DCNN for the defect recognition tasks.

It is a trend to deploy those algorithms on UAVs to realize real-time power transmission line condition screening, yet is hindered because of two main reasons. Firstly, the methods mentioned above [6] require high computational costs, and the accuracy of detection methods can not be guaranteed, so that the real-time video is needed to transmitted from UAVs to the local server to ensuring, which causes much energy wasting. In addition, the *data island* phenomenon that is the small-scale, inaccessible, inconsistent, and of poor quality fine-annotated data, hampers the deployment of those mentioned deep learning models in practical applications scenarios.

In this paper, we propose a novel cloud edge collaborative intelligence method for insulator string defect-recognition to mitigate those challenges, as Fig. 1 shown. Specifically, the whole framework is divided into two parts. In edge devices (UAVs), we locate the insulator with an anchor-free object detector, which only needs labels of the location of insulator but fault part. It is simple and inexpensive to prepare large-scale training data. When the insulator is detected, the image will be transported to the cloud server and predicted by the

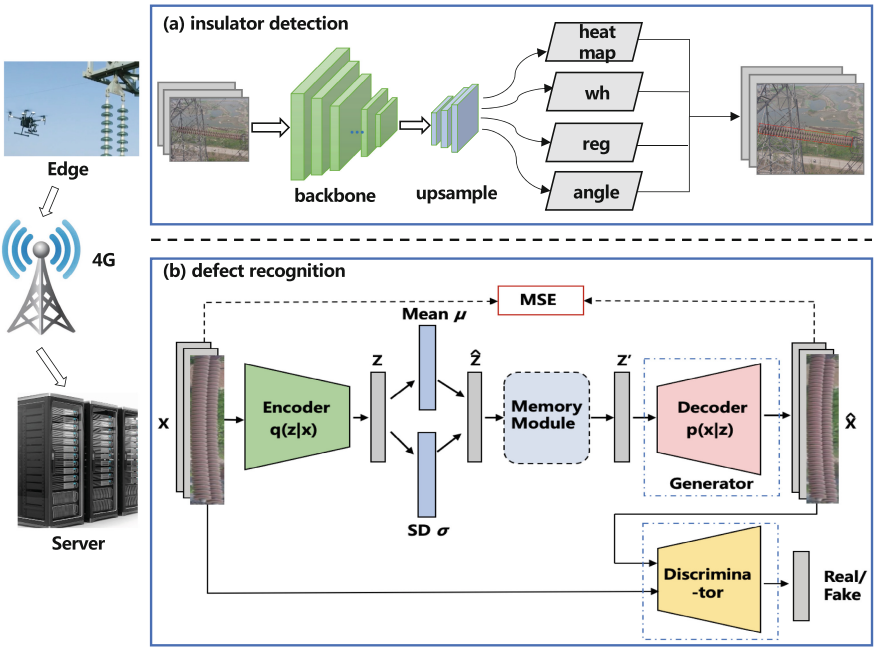

Fig. 1. The proposed cloud edge collaboration framework includes two parts: (a) insulator detection (b) defect recognition. The solid line is the forward propaganda and the dashed line represents the back propaganda.

defect recognition network following. The main contributions of this work are the following:

1) We deploy an anchor-free object detector to locate the insulator on the UAVs. We improve the CenterNet [13] with an extra angle regression, for reducing the energy consumption and predicting the insulator string with the oriented bounding box, respectively.

2) To address the scarcity of faulty insulator data, a generative insulator defect detection model based on the autoencoder with a generator-discriminator pattern is proposed. Particularly, we introduce the variational memory encoder-decoder architecture to model defect-free insulator data distribution. It mitigates the overly-smooth problem of traditional variational autoencoder (VAE). Furthermore, the adversarial strategy is employed to regularize the generated data space with input data space.

The remainder of this paper is structured as follows. Section 2 presents the related work about insulator anomaly detection using CNNs. Section 3 introduces the proposed architecture of the cloud edge collaborative network. Section 4 presents the results of the experiments and provides comparisons to other work. Finally, the conclusions are demonstrates in Sect. 5.

2 Related Work

The availability of large-scale data sets and the high performance of GPU have enabled deep learning to develop rapidly, which powers many computer vision filed. Likewise, the application of deep learning methods for condition monitoring of transmission line equipment is gaining momentum. The most common method for insulator condition screening usually extracts the insulator string from the complex background first and then identifies the defect location. There are many works [7,14] adopt the representative deep convolutional network such as Fast-RCNN and Faster-RCNN to locate the insulators, but it is hard to realize real-time inspection due to their complicated calculation. [9] et al. detect the insulator string from coarse to fine with traditional method and CNN respectively, and then take advantage of the segmentation result in the previous step to identify the defect position. A cascading architecture is utilized in [6,16], which deploy different CNN for the insulator location and defect-recognition task, and both works contain a crop operation between two different networks.

The generative anomaly detection models attract lots of attention, it only needs normal samples, which alleviate the bottleneck of scarce defective insulator images. Thus, those methods avoid being over-fitting problem under the few-shot learning. For example, Kang et al. [15] integrate a deep material classifier and a deep denoising autoencoder together into a multitask learning framework and only need normal insulator samples for training a defect detection network. Deep autoencoder [22,23] is basically consisted of an encoder that able to extract the high-dimensional representation of input images, and a decoder to reconstruct the encoded data. The autoencoder(AE) technique has been extensively used now for anomaly detection in the unsupervised setting. But there exists a problem that it may perform too "well", that leading to a "great" reconstruction of anomalies. Exiting VAEs-based work [17], however, are observed can only learn an ambiguous model, which exists the same issues like the standard AE, due to the lack of constraints. Furthermore, MemAE [18][19] is introduced to alleviate this problem based on the reconstruction of the most relevant item of the input in the memory module to enlarge the difference of the normal sample and novelty. Yet it ignores the local feature learning and is limited by the capability of storage, the *over-smooth* [20] problem is arisen by utilizing the mean square loss function with averaging effect. The adversarial autoencoder networks [25,26] blends the autoencoder architecture with the adversarial loss concept introduced by GAN [24]. Inspired by these works, we convert the insulator defect detection to an unsupervised anomaly detection problem, and an implicate-explicate combined generative insulator defect detection model based on the autoencoder with an adversarial pattern is introduced.

3 Method

The whole framework consist of two phases: insulator detection on the edge device and defect recognition on cloud, and they are supposed to be processed

separately. In the following, we will introduce an anchor-free oriented insulators detector and reconstruction-based defect detection network, respectively.

3.1 Insulator Detection on the Edge Device

For the purpose of reducing energy consumption, we introduce the CenterNet [13] which is a simpler and efficient anchor-free keypoint-based detector compared with corresponding bounding box-based detectors. The common object detection algorithm heavily relies on the time-consuming post-grouping process, which is not suitable for deployment on the edge device. Moreover, it is observed that the aspect ratios of insulator string are mostly larger than general objects, which may be even larger than 20. The larger aspect ratios lead to a bad performance in the fault detection task because the predicted regions contain much meaningless background information. In this paper, we extend Zhou's work [13] to the oriented insulator string detection task.

Specifically, our network use the Deep Layer Aggregation (DLA) [31] as backbone, whose parameters are less than ResNet50. Feature maps for prediction are fused from multi-layer of backbone network. We build it on a U-shaped architecture, whose size is 4 times smaller than the input image. The progressively combination of shallow and deep layer provides a comprehensive fine and coarse granularity information. In particular, given a RGB image as input $I \in R^{W \times H \times 3}$, where W and H represents the width and height, respectively, the output feature map $X \in R^{\frac{W}{4} \times \frac{H}{4} \times C}$ (C denotes the channel) is then fed into our four branch heads: heatmap ($H \in R^{\frac{W}{4} \times \frac{H}{4} \times 1}$), offset ($O \in R^{\frac{W}{4} \times \frac{H}{4} \times 2}$), box-parameter ($B \in R^{\frac{W}{4} \times \frac{H}{4} \times 2}$), and angle map ($A \in R^{\frac{W}{4} \times \frac{H}{4} \times 1}$).

The grand truth is denoted as (x, y, w, h, α), where x, y denotes the centers' coordinates and w, h, α is the weight, height, and angle. Following, we use the focal loss to train the heatmap:

$$L_H = -\frac{1}{N} \sum_i \begin{cases} (1 - H_i)^{\alpha} log(H_i) & if \hat{H}_i = 1 \\ (1 - \hat{H}_i)^{\beta} H_i^{\alpha} log(1 - H_i) & otherwise, \end{cases} \tag{1}$$

where $\hat{H}_i$ refer to the Ground Truth and H_i is predicted heatmap values, α and β are the hyper-parameters. The offset between the scaled center point and the predicted is:

$$o = (\frac{x}{4} - \frac{\hat{x}}{4}, \frac{y}{4} - \frac{\hat{y}}{4}). \tag{2}$$

And the offset is trained by minimizing a smooth $L1$ Loss:

$$L_O = \frac{1}{N} \sum_i Smooth_{L_1}(o_i - \hat{o}_i). \tag{3}$$

Likewise, the box parameters $b_i = [w_i, h_i]$ and angle α_i are trained with offset o_i using smooth $L1$ Loss, which denotes as L_B and L_A, respectively. Finally, the network is optimized by the sum of L_H, L_O, L_B, and L_A.

3.2 Defect Recognition on the Cloud Server

In this paper, we propose an adversarial Variational memory autoencoder network. Opposite of object detection-based anomaly detection methods, this paper utilizes an implicit method based on Variational autoencoder (VAE) architecture to model normal data distribution. It can alleviate the dilemma of defining encompasses of a real-world high-diversity outlier, owing to the abnormal insulator sample is hard and costly to collect. In the following part, we firstly provide the structure of Variational autoencoder architecture; then we introduce memory module architecture; in the end, we will give the whole framework process combining Variational memory autoencoder and discriminator and the corresponding loss functions.

Variational Memory Autoencoder consists of three components: (i) the encoder network for learning a meaningful latent representation of the input normal data on its manifold space; (ii) the Variational part for learning a data generating distribution, and the memory module which given random samples from latent space distribution, it can retrieve the most homogeneous item; (iii) the decoder network for reconstructing the item from the memory module. In the training phase, the parameter of the network only trained on normal data. In the inference stage, the memory module is fixed. Therefore, the normal samples can be reconstructed well with its homogeneous memory item while the defective insulator string leads to a high reconstruction error due to it has to retrieve the most relevant normal item.

The objective of the encoder is to learn an approximation to the posterior distribution $p(z|x)$ of defect-free data, however, it is cumbersome and intractable to analytically approach, due to the high computationally expensive sampling of Markov Chain Monte Carlo (MCMC) methods. Alternatively, the Variational autoencoder approximates the posterior distribution $p(z|x)$ as a family of possible distribution $p(z)$ which is able to be generated by our controllable data, such as Gaussian distribution, Poisson, binomial, etc. In this paper, we follow the work [17] which uses the Gaussian distribution $p(z) = Normal(0, 1)$. So that, we maneuver the approximation of $p(z|x)$ as $p(z)$. In our task, only given the normal samples, the encoder network models its probability distribution $p(z|x)$:

$$p(z|x) = \frac{p(x|z)p(z)}{p(x)} = \frac{p(x|z)p(z)}{\sum_z p(x|z)p(z)}. \tag{4}$$

In the second stage, it concludes two modules: variational function and memory table. The variational function taken the mean and standard deviations of the latent embedding feature of the current input image from the encoder forms data generating distribution $p(z|x)$. Essentially, the variational parameter is independent of each other, therefore, we can multiply together to give a joint probability:

$$p(z|x) \approx p(z) = \prod_{i=1}^{N} p_i(z_i). \tag{5}$$

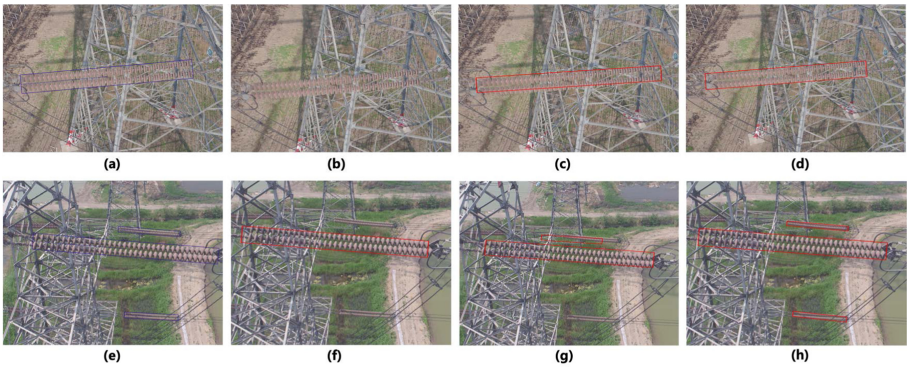

Fig. 2. Insulator string detection results comparison

We employ Kullback-Leibler (KL) divergence to measure their similarity:

$$\begin{aligned} KL(p(z)||p(z|x)) &= \mathbb{E}_{z\sim p} logp(z) - \mathbb{E}_{z\sim p} logp(z|x) \\ &= \mathbb{E}_{z\sim p} logp(z) - \mathbb{E}_{z\sim p} logp(z,x) + logp(x). \end{aligned} \tag{6}$$

Through minimize KL divergence, we achieve approximation $p(z|x)$ as $p(z)$. The new feature vector $\hat{z}$ is sampled from the "learned" latent space $p(z|x)$, which is feed into our memory module and stored at the memory slots matrix $M = \{m_1, m_2, ..., m_i, ..., m_N\} \in \mathbb{R}^{N\times F}$, where N means the number of memory slots and F represents dimension of every latent feature that is memorized. Simultaneously, the similarity coefficients W_i is denoted as cosine distance between input $\hat{z}$ and the memory item m_i as:

$$W_i = \frac{\hat{z} \cdot m_i^T}{||\hat{z}|| \cdot ||m_i||}. \tag{7}$$

In the end, following [18], the final embedding feature z' is retrieved and feed into decoder with soft address method with the similarity coefficients W_i:

$$z' = \sum_{i=1}^{N} \frac{exp(W_i)}{\sum_{i=1}^{N} exp(W_i)} m_i. \tag{8}$$

$$L_D = logD(x) + log(1 - D(G(z'))) \tag{9}$$

The decoder network $p(x|z')$ learns to reconstruct the input space distribution given latent representation distribution. The architecture of decoder is symmetrical with encoder network. In the sum, the loss function of variational memory autoencoder (L_{VMAE}) consists two parts, reconstruction loss and KL:

$$L_{VMAE} = MSE(x, \hat{x}) + KL(p(z)||p(z|x)), \tag{10}$$

where MSE is the mean square error between input and reconstructed images.

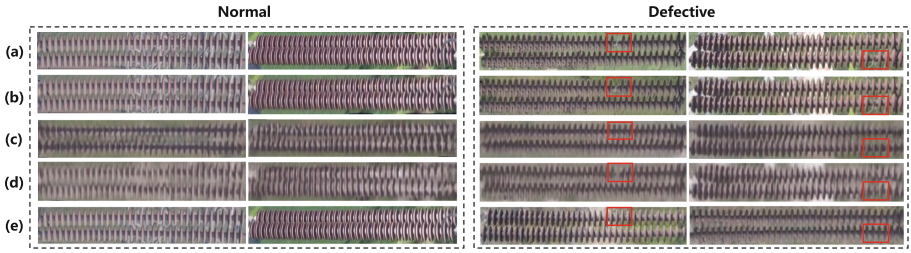

Fig. 3. The comparison of reconstruction normal insulator (left), defective insulator (right) of our method and other baselines. (a) input samples (b) reconstruction of AE (c) reconstruction of MemAE [18] (d) reconstruction of Variational AE [17] (e) reconstruction of our proposed method (Color figure online)

Adversarial Discriminator. Moreover, autoencoder is inherently blurry, inspired by the Ganomaly [27], we introduce the discriminator to improve the reconstruction image quality and senses. The objective of the discriminator network is to classify the input x and the reconstructed $\hat{x}$ as real or fake, respectively. The discriminator is constructed by multi-layer perception neural networks. In addition, the decoder network in this paper is treated as a generator, which reconstructs an image from the latent space in order to interfere with the judgment of the discriminator network. The discriminator can be trained by minimizing the loss function as: where D denotes the discriminator function, G represents the generator function. x means the input image and z' is the output of the variational memory autoencoder. Furthermore, the generator is adversarial trained by maximizing the second part of the discriminator loss function:

$$L_G = log(1 - D(G(z'))). \tag{11}$$

4 Experiments

Our method for insulator string detection and defect recognition are evaluated in this section independently. The data set we used comes from [6], which includes 600 high resolution normal insulator string images and 248 images with bunch-drop defect. The dataset are captured by an UAV with a DJI M200 camera. All positive samples includes one or more anomaly-free insulators. Negative cases are defective insulator images. Besides, the experiment is conducted based on the configuration as: Intel Core i7-7600, and GTX 1080 GPU with 8-GB memory.

4.1 Implementation Detail

For the insulator detection experiment, the fully convolutional upsampling version of DLA is utilized to obtain an informative feature map. Following the work in [13], the original convolution at each upsampling layer is replaced by 3×3 deformable convolution. The input image is resized to 512×512 before sending

to the detection network. And then a high-resolution feature map (128×128) can be acquired. Moreover, a series of data augmentation such as cropping, random flip, and scaling is used to increase the robustness of our model. We train our detection model with 8 batch-size, and the learning rate is set as 2e–4 which is supposed to drop 10 times at 90 and 120 epochs. In addition, we use Adam [29] to optimize the objective function. For the defect recognition experiment, we cropping and rotating the inspection bounding box, which is predicated on the normal insulator data set, to a horizontal level. And then resizing the result to 68×500 before feeding into the autoencoder network. Meanwhile, we build an encoder network with ResNet50, and the decoder is symmetrical to the encoder. The memory size N of the memory module is set as 1000. And we train with batch-size 8 and learning rate 10e–4 for every 500 epochs. Furthermore, we still utilize Adam as the optimizer in this experiment.

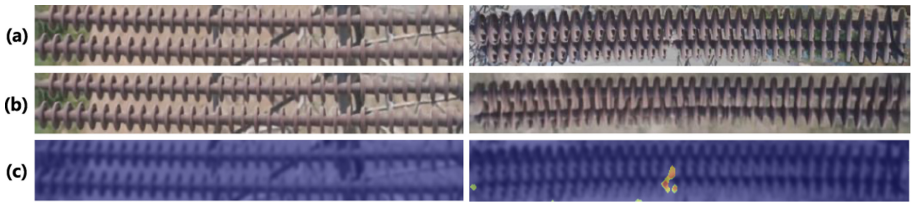

Fig. 4. The discrepancy between input samples and reconstruction result of our method in normal sample (left) and defective sample (right) (a) input samples (b) reconstruction result (c) the discrepancy. (Color figure online)

4.2 Experiment Results

Figure 2 gives the insulator detection results using different methods. (a), (e) indicate the manual label, and the middle two columns are predicted by the CenterNet-ResNet18 and CenterNet-ResNet50 respectively. We yield the best performance utilizing the CenterNet-Dla34 as (d) and (h) shown, which locate the insulator string with high accuracy. Besides, the precision, recall, F1 score, parameter, and testing speed comparison are reported at Table 1. The first three rows are tested with anchor-based detection methods, and the remaining models are all based on CenterNet. From the reported results, we can see that under the high inference speed, our framework achieves superior precision and recall.

Figure 3 compares the reconstruction images generated by different methods, and for better visualization, we enclose the defective area by red lines. The standard AE "generalize" so well on both normal and defective image as (b) represent, thus it can not recognize the abnormal data according to the difference of reconstruction error. Moreover, the generalization capability of MAE is unsatisfied, which means it may only perform well on trained data. The VAEs learn the generating distribution of training data so that it is able to reconstruct a more normal-like image. But as shown in (d), the reconstruction images are too

Table 1. Detection performance for different methods.

Method	Precision	Recall	F1	Parameter	Testing speed
Faster R-CNN [7]	0.791	0.573	0.665	138M	180 ms/image
ILN-VGG16 [6]	0.904	0.966	0.934	136M	115 ms/image
Cascaded DNN [30]	0.882	0.861	0.871	–	387 ms/image
CenterNet-ResNet18	0.876	0.571	0.691	14.91M	34 ms/image
CenterNet-ResNet50	0.910	0.455	0.607	31.16M	48 ms/image
CenterNet-DLA34 (ours)	**0.946**	**0.864**	**0.903**	20.32 M	52 ms/image

Table 2. The performance of our model compared with the SOTA methods.

Method	Precision	Recall	F1
Autoencoder	0.410	0.516	0.457
Memory autoencoder [18]	0.512	0.677	0.583
Ganomaly [27]	0.509	0.903	0.651
Variational autoencoder [17]	0.704	0.954	0.810
Ours	**0.968**	**0.985**	**0.9769**

blurry to distinguish the defect region. The bottom row (e) indicates the output of our proposed model, which efficiently mitigates the issues mentioned above. Besides, the absent piece of defect insulator has been 'patched' after reconstruction. In this case, the faulty insulator is able to get a higher reconstruction error compared with the normal insulator.

Figure 4 shows the discrepancy between the input image and reconstruction image. The first column represents the normal insulator, and the second column is the defective insulator with a bunch-drop fault. The defective region is highlighted with bright color, and the normal part maintains a dark blue color as (c) shown. From the discrepancy result, we can easily locate the fault. Table 2 compare the value of precision, recall, and F1 score between four methods with our proposed model. The standard autoencoder without any constraints gets the lowest precision and recall score. Besides, simply appending the memory module and variation process achieve no significant improvement. The precision of Ganomaly can not meet the detection requirement. It shows that our method yields the best performance with the result of 0.9688, 0.9853, and 0.9769 respectively which is highlighted in bold in Table 2.

5 Conclusion

In this paper, a cloud edge collaborative insulator string anomaly detection framework is proposed. We depart the defect inspection task into two independent procedures: (1) insulator detection; (2) defect recognition. The former step is carried out by improving an anchor-free detector called CenterNet, which is

able to alleviate the calculation burden of the edge device. Moreover, we introduce an adversarial autoencoder model with a variation process and memory module for defect recognition. The experiment results proof that the proposed framework can achieve state-of-the-art performance on abnormal detection. In further work, we will explore the knowledge distillation methods on edge devices to prune the network and anomaly detection generative model on the cloud side.

Acknowledgment. This work was supported in part by the National Natural Science Foundation of China under Grants 62027810, 61733004, National Key RD Program of China under Grant 2020YFB1712600, and the Hunan Provincial Natural Science Foundation of China under Grant 2020JJ5090, 2018GK2022, 2017XK2102, and China Postdoctoral Science Foundation under Grant BX20200122 and 2020M682555.

References

1. Han, J., et al.: A method of insulator faults detection in aerial images for high-voltage transmission lines inspection. Appl. Sci. **9**(10), 2009 (2019)
2. Zhong, H., Miao, Z., Wang, Y., et al.: A practical visual servo control for aerial manipulation using a spherical projection model. IEEE Trans. Ind. Electron. **67**(12), 10564–10574 (2019)
3. Zhong, H., Wang, Y., et al.: Circumnavigation of a moving target in 3D by multi-agent systems with collision avoidance: an orthogonal vector fields-based approach. Int. J. Control Autom. Syst. **17**(1), 212–224 (2019)
4. Tiantian, Y., et al.: Feature fusion based insulator detection for aerial inspection. In: 2017 36th Chinese Control Conference (CCC), pp. 10972–10977. IEEE (2017)
5. Liao, S., An, J.: A robust insulator detection algorithm based on local features and spatial orders for aerial images. IEEE Geosci. Remote Sens. Lett. **12**(5), 963–967 (2014)
6. Tao, X., Zhang, D., Wang, Z., et al.: Detection of power line insulator defects using aerial images analyzed with convolutional neural networks. IEEE Trans. Syst. Man Cybern. Syst. **50**(4), 1486–1498 (2018)
7. Ren, S., He, K., Girshick, R., et al.: Faster R-CNN: towards real-time object detection with region proposal networks. IEEE Trans. Pattern Anal. Mach. Intell. **39**(6), 1137–1149 (2016)
8. Liu, D., Zeng, X., Wang, Y.: Edge-computing-driven autonomous ubiquitous internet of things in electricity: architecture and challenges. In: 2019 IEEE 3rd Conference on Energy Internet and Energy System Integration (EI2), pp. 456–461. IEEE (2019)
9. Song, C., et al.: A cloud edge collaborative intelligence method of insulator string defect detection for power IIoT. IEEE Internet Things J. **8**(9), 7510–7520 (2020)
10. Zhao, Z., Xu, G., Qi, Y., et al.: Multi-patch deep features for power line insulator status classification from aerial images. In: 2016 International Joint Conference on Neural Networks (IJCNN), pp. 3187–3194. IEEE (2016)
11. Wang, W., Wang, Y., Han, J., et al.: Recognition and drop-off detection of insulator based on aerial image. In: 2016 9th International Symposium on Computational Intelligence and Design (ISCID), vol. 1, pp. 162–167. IEEE (2016)
12. Zhai, Y., Chen, R., Yang, Q., et al.: Insulator fault detection based on spatial morphological features of aerial images. IEEE Access **6**, 35316–35326 (2018)

13. Zhou, X., Wang, D., Krähenbühl, P.: Objects as points. arXiv preprint arXiv:1904.07850 (2019)
14. Ma, L., Xu, C., Zuo, G., et al.: Detection method of insulator based on faster R-CNN. In: 2017 IEEE 7th Annual International Conference on CYBER Technology in Automation, Control, and Intelligent Systems (CYBER), pp. 1410–1414. IEEE (2017)
15. Kang, G., Gao, S., Yu, L., et al.: Deep architecture for high-speed railway insulator surface defect detection: denoising autoencoder with multitask learning. IEEE Trans. Instrum. Meas. **68**(8), 2679–2690 (2018)
16. Ling, Z., Qiu, R.C., Jin, Z., et al.: An accurate and real-time self-blast glass insulator location method based on faster R-CNN and U-net with aerial images. arXiv preprint arXiv:1801.05143 (2018)
17. Kingma, D.P., Welling, M.: Auto-encoding variational bayes. arXiv preprint arXiv:1312.6114 (2013)
18. Gong, D., Liu, L., Le, V., et al.: Memorizing normality to detect anomaly: memory-augmented deep autoencoder for unsupervised anomaly detection. In: Proceedings of the IEEE/CVF International Conference on Computer Vision, pp. 1705–1714 (2019)
19. Chen, Y., Zhang, H., Wang, Y., et al.: MAMA net: multi-scale attention memory autoencoder network for anomaly detection. IEEE Trans. Med. Imaging **40**(3), 1032–1041 (2020)
20. Zhao, H., Gallo, O., Frosio, I., et al.: Loss functions for image restoration with neural networks. IEEE Trans. Comput. Imaging **3**(1), 47–57 (2016)
21. Wang, X., Du, Y., Lin, S., Cui, P., Shen, Y., Yang, Y.: Advae: a self-adversarial variational autoencoder with gaussian anomaly prior knowledge for anomaly detection. Knowl.-Based Syst. **190**, 105187 (2020)
22. Zhou, C., Paffenroth, R.C.: Anomaly detection with robust deep autoencoders. In: Proceedings of the 23rd ACM SIGKDD International Conference on Knowledge Discovery and Data Mining, pp. 665–674 (2017)
23. Chen, J., Sathe, S., Aggarwal, C., Turaga, D.: Outlier detection with autoencoder ensembles. In: Proceedings of the 2017 SIAM International Conference on Data Mining, pp. 90–98. SIAM (2017)
24. Goodfellow, I., et al.: Generative adversarial nets. In: Advances in Neural Information Processing Systems, pp. 2672–2680 (2014)
25. Makhzani, A., Shlens, J., Jaitly, N., et al.: Adversarial autoencoders. arXiv preprint arXiv:1511.05644 (2015)
26. Chen, Y.: Graph-embedding Enhanced Attention Adversarial Autoencoder. University of Pittsburgh (2020)
27. Akcay, S., Atapour-Abarghouei, A., Breckon, T.P.: GANomaly: semi-supervised anomaly detection via adversarial training. In: Jawahar, C.V., Li, H., Mori, G., Schindler, K. (eds.) ACCV 2018. LNCS, vol. 11363, pp. 622–637. Springer, Cham (2019). https://doi.org/10.1007/978-3-030-20893-6_39
28. Donahue, J., Krahenbuhl, P., Darrell, T.: Adversarial feature learning. In: International Conference on Learning Representations (ICLR) (2016)
29. Kingma, D.P., Ba, J.: Adam: a method for stochastic optimization. ICLR (2014)
30. Chen, J., Liu, Z., Wang, H., Núñez, A., Han, Z.: Automatic defect detection of fasteners on the catenary support device using deep convolutional neural network. IEEE Trans. Instrum. Meas. **67**(2), 257–269 (2018)
31. Yu, F., Wang, D., Shelhamer, F.: Darrell. Deep layer aggregation. In: CVPR (2018)